Oxidation of TDMQ20, a Specific Copper Chelator as Potential Drug Against Alzheimer's Disease

Michel Nguyen, Youzhi Li, Anne Robert, Yan Liu, Bernard Meunier

Oxidation of TDMQ20, a Specific Copper Chelator as Potential Drug Against Alzheimer's Disease

Michel Nguyen,[a] Youzhi Li,[b] Anne Robert,*[a] Yan Liu,*[b] and Bernard Meunier*[a,b]

[a] Dr. M. Nguyen, Dr. A. Robert, Dr. B. Meunier
Laboratoire de Chimie de Coordination du CNRS, Inserm ERL 1289,
205 route de Narbonne, 31077 Toulouse cedex, France.
E-mail: anne.robert@lcc-toulouse.fr, bmeunier@lcc-toulouse.fr
[b] Dr. Y. Li, Dr. Y. Liu
School of Chemical Engineering and Light Industry, Guangdong University of Technology,
Higher Education Mega Center, Guangzhou 510006, P. R. China.
E-mail: yanliu@gdut.edu.cn

Supporting information for this article is given via a link at the end of the document.

Abstract: Developed as a regulator of copper homeostasis in the brain of patients affected by Alzheimer's disease (AD), TDMQ20 is a specific copper(II) chelator able to restore short term memory in AD mice. To anticipate on metabolic studies of this drug-candidate, here we report the catalytic oxidation of TDMQ20 by a biomimetic system reminiscent of P450 oxidation, using a metalloporphyrin and hydrogen persulfate as oxidant. Oxidation products were mainly characterized by HPLC with UV-visible spectrometry or high-resolution mass spectrometry detection. In these conditions, TDMQ20 was readily oxidized by aromatic hydroxylation, oxidation of 1,4-diphenol or 1,4-aminophenol to 1,4-quinone or quinone-imine, respectively, or oxidative chlorination. These putative metabolites were water-soluble, suggesting that the drug-candidate might be easily metabolized and excreted *in vivo*.

Introduction

With the increase in life expectancy, Alzheimer's disease (AD), age-related disease, is one of the major public health issues in the world. Unfortunately, very few treatments have been approved until recently,[1,2] and these drugs are not curative, offering only short-term symptomatic relief, a high level of side effects and questionable efficiency/cost ratios.[3] Then, there is an urgent need to enlarge the drug spectrum with molecules acting by different mechanisms, in order to stop the neurodegenerative process and the cognitive decline at the early stages of the disease. The destruction of neurons in brains affected by AD has been attributed to an oxidative stress mainly caused by rupture of the homeostasis of redox-active metal ions, such as copper and iron, trapped by β-amyloid peptide (Aβ).[4-6] Then, we designed specific copper chelators named TDMQ (Scheme 1), able to inhibit the catalytic reduction of dioxygen produced by copper-loaded amyloids (Cu-Aβ).[4,7-9] Based on an 8-aminoquinoline skeleton with a chelating side chain at C2, these ligands have the required structure to generate Cu(II)-TDMQ complexes with a tetradentate N4-square planar scaffold.[10] Due to this coordination pattern, TDMQ20 (Scheme 2), exhibits a high chelation specificity for Cu(II) with respect to Cu(I) or to other divalent biologically relevant metal ions such as Fe(II) or Zn(II).[11,12] Due to its high affinity for Cu(II), TDMQ20 is able to transfer copper from Cu-amyloid complexes to the Cu-glutathione complex which is a natural provider of copper to copper proteins, without disturbing the activities of copper proteins such as Cu,Zn-SOD or tyrosinase.[13] Oral administration of TDMQ20 to three different murine models of AD indicated that this specific regulator of copper homeostasis reduced the oxidative stress in mouse cortex, and was able to rescue the declarative memory and to inhibit cognitive impairment of the early stages of AD, without any detectable toxic effect.[14,15] TDMQ20 can therefore be considered as a promising drug-candidate. In this context, to document the possible oxidative metabolism of this drug, we investigated its oxidation by biomimetic systems.

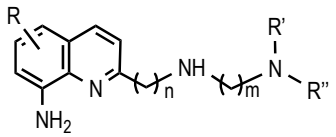

Scheme 1. General structure of the Cu(II) specific TDMQ chelators.

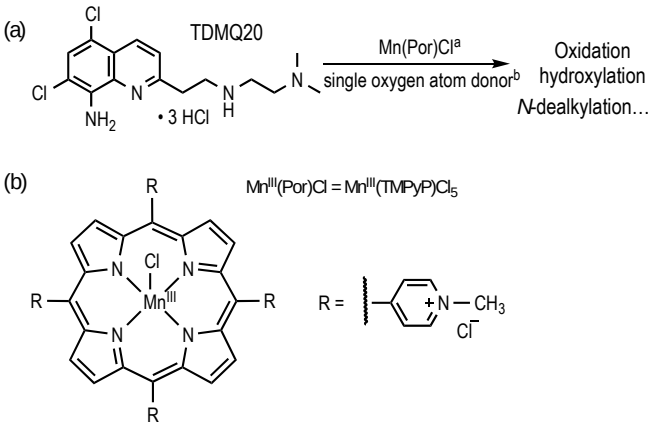

[a] Mn(Por)Cl stands for a metalloporphyrin complex as catalyst, for example $Mn(TMPyP)Cl_5$. [b] The single oxygen atom donor is hydrogen persulfate (HSO_5^-) or meta-chloroperbenzoic acid (mCPBA).

Scheme 2. Biomimetic oxidation of TDMQ20 using a manganese porphyrin catalyst associated to hydrogenpersulfate or *m*-chloroperbenzoic acid as oxygen atom donor.

The biomimetic oxidation of drugs by redox-active metalloporphyrin catalysts associated with a single oxygen atom donor has been reported to efficiently mimic the biotransformation performed *in vivo* by cytochromes P450 or peroxidases, two families of major enzymes involved in xenobiotic metabolism.[16-18] In fact, these catalytic systems can efficiently oxidize a variety of substrates and perform, among other reactions, biologically relevant hydroxylation of saturated structures, oxidation of aromatics, or *N*-demethylation of substituted amines. We report here the catalytic oxidation of TDMQ20 in such oxidative conditions.

Results and Discussion

The selection of the different metalloporphyrin catalysts and associated oxidants was based on their known abilities to mimic the reactions mediated by cytochrome P450 enzymes. The activation of metal complexes of porphyrins by single oxygen atom donors (hypochlorite, hydrogen persulfate, *meta*-chloroperbenzoic acid, magnesium monoperoxyphthalate...), involves a highly electrophilic metal-oxo active species which is reminiscent of cytochrome P450 active species generated in the presence of dioxygen associated with NADPH/P450 reductase.[16] The general equation of these catalytic biomimetic reactions is depicted in Scheme 2. First, the non-catalytic oxidation of base form of TDMQ20 by *m*-chloroperbenzoic acid (mCPBA) or tetrabutylammonium hydrogen monopersulfate (NBu_4HSO_5) was carried out, in order to characterize expected *N*-oxide derivatives of the drug. Then, oxidation of TMDQ20 was carried out using manganese(III) tetramethylpyridiniumylporphyrin, pentachloride [$Mn(TMPyP)Cl_5$, MnTMPyP for short] as catalyst and potassium hydrogen persulfate ($KHSO_5$) as oxidant in a acetonitrile/water mixture.[16] To get a fairly broad overview of the possible metabolites of TDMQ20, various oxidative conditions were explored: different oxidants, aqueous or organic media, variable concentrations of TDMQ20 (in the range 50 µM-1 mM) and reaction times, etc. All reactions were monitored by HPLC with UV-visible detection at 260 and 340 nm, and by LC-MS [TDMQ20: t_R = 16.8 min, *m/z* = 327.1 amu (MH^+)].

Oxidation of TDMQ20 by mCPBA

In the absence of catalyst, TDMQ20 or its base form were readily oxidized in aqueous acetonitrile or in dichloromethane, respectively. For example, oxidation of TDMQ20 (base form,10 mM) by mCPBA (1.2 molar equiv) in CH_2Cl_2 resulted in a 99 % conversion after 15 min, and products **1** (t_R = 18.6-18.7 min) and **2** (t_R = 21.7 min), were characterized by mass increments of +16 amu and +32 amu, respectively (Figure S1). The structure of these products resulting from *N*-oxidation of the distal tertiary amine or *N*-oxidation of the two amines of the side chain, respectively, were fully characterized by NMR after chromatographic purification (Schemes 3 and 4). The ^{13}C chemical shift of the terminal N–CH_3, detected at 45.6 ppm in TDMQ20 (base) was downfield shifted by +14.1 and +13.2 ppm in compounds **1** and **2**, respectively (N–CH_3 detected at 59.8 ppm and 58.8 ppm in **1** and **2**, respectively, see Scheme 3). The signal of the distal methylene group CH_2–$N(CH_3)_2$ was detected at 69.6 and 69.0 ppm in **1** and **2**, respectively, also shifted by more than 10 ppm with respect to TDMQ20 (58.7 ppm). In addition, ^1H chemical shifts of N–CH_3 and CH_2–$N(CH_3)_2$ were shifted by 1.0 ± 0.1 ppm with respect to the corresponding signals of TDMQ20. These results are fully consistent with *N*-oxidation of the distal site. The carbon spectrum of **1** exhibited a low shift of Quin–CH_2-CH_2-N (48.6 ppm) and Quin–CH_2-CH_2-N-CH_2 (44.8 ppm), with $\Delta\delta$ = 0.1 ppm and –2.3 ppm, respectively, compared to TDMQ20 (48.6 and 47.1 ppm, respectively), strongly suggesting that no reaction occurred at the proximal amine. Conversely, the spectrum of **2** exhibited strongly downfield shifted resonances for Quin–CH_2-CH_2-N (59.4 ppm) and Quin–CH_2-CH_2-N-CH_2 (55.6 ppm) [$\Delta\delta$ = +10.8 ppm and +8.5 ppm, respectively, compared to TDMQ20 base] that are significant of a second *N*-oxidation of the molecule on this proximal nitrogen. In addition, the resonance of carbon atoms of the quinoline nucleus were detected at very close values in TDMQ20 base, **1** and **2** ($\Delta\delta \leq 0.5$ ppm), indicating that no oxidation occurred on the aromatic moiety of TDMQ20 (Scheme 3).

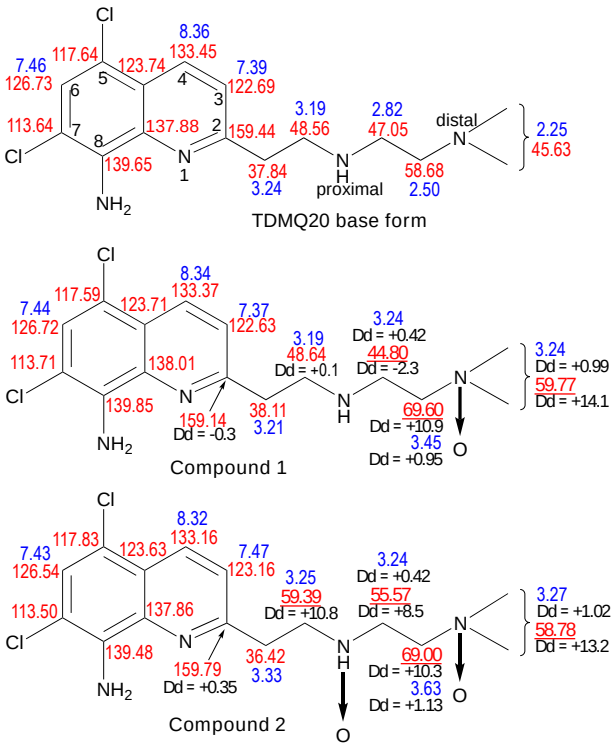

Scheme 3. Results of 2D-NMR characterization of TDMQ20 base, and N-oxide derivatives 1 and 2 in $CDCl_3$. Blue and red labels stand for ^1H and ^{13}C chemical shifts, respectively; black labels $\Delta\delta$ stand for the difference between ^1H or ^{13}C chemical shifts δ of **1** or **2**, and the corresponding δ values of TDMQ20 base.

The UV-visible characteristics of isolated compound **1** were very similar to that ones of TDMQ20, with λ_{max} = 261 and 345 nm, and ε_{260} = 30,000 L x mol^{-1} x cm^{-1}. Consequently, the yields of products **1** and **2** were calculated directly using the UV-vis trace of HPLC chromatograms. In these conditions, after 15 min, the yields of **1** and **2** were 70% and 7%, respectively, with respect to the starting amount of TDMQ20.

Oxidation of TDMQ20 by hydrogen persulfate (NBu_4HSO_5 or $KHSO_5$)

When TDMQ20 (base form,10 mM) was oxidized by hydrogen persulfate (1 mol equiv, NBu_4HSO_5) instead of mCPBA in CH_2Cl_2, the conversion of TDMQ20 was 57% after 10 min. The *N*-oxide derivative **1** was detected as main product (yield = 52% with respect to starting amount of TDMQ20). The di-*N*-oxide **2** was also detected in very low yield (≤ 2%). In the presence of an excess of oxidant, (2 mol equiv), compound **2** was no more detected. In these conditions, a minor product **3** was detected but not isolated (t_R = 20.3-20.4 min, 2% yield). Its chromatographic peak exhibited maximum wavelengths at 260-261 nm and 345 nm, indicating that the 8-aminoquinoline ring of TDMQ20 was unchanged, and a *m/z* value = 256.0 amu, that should correspond to oxidative dealkylation of the proximal secondary amine (Scheme 4).

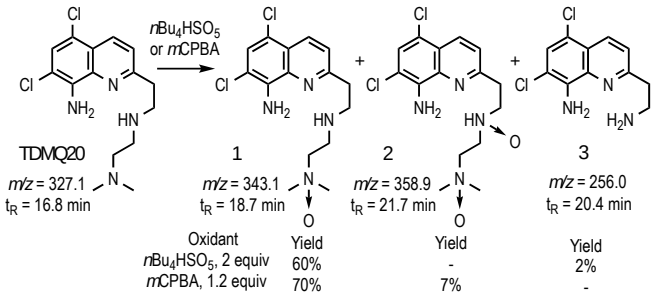

Scheme 4. Oxidation of TDMQ20 by tetrabutylammonium hydrogenpersulfate or by *m*-chloroperbenzoic acid in CH_2Cl_2, in the absence of catalyst, after 15 min.

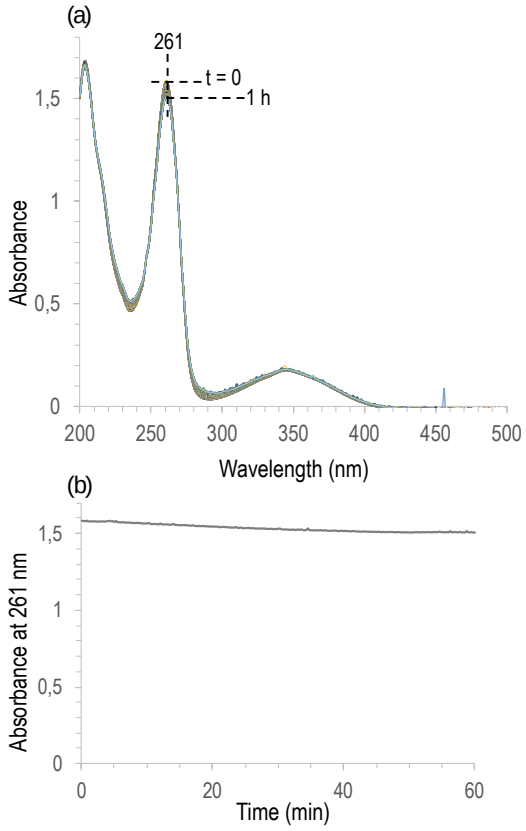

Figure 1. (a) UV-visible kinetic spectra of oxidation of TDMQ20 (50 μM) by $KHSO_5$ 4 mol equiv in H_2O/CH_3CN, 1/1, v/v; (b) Absorbance at 261 nm according to the reaction time after addition of $KHSO_5$.

UV-vis monitoring of the oxidation of TDMQ20 (50 μM) by $KHSO_5$ (4 mol equiv) in aqueous acetonitrile (CH_3CN/H_2O = 1/1, v/v) confirms that the spectrum of the reaction mixture did not significantly change upon oxidation of TDMQ20 after 1 h (Figure 1).

Then, the substrate conversion and yield of products **1**-**3** reported in Scheme 4 were roughly calculated from the areas of the HPLC peaks upon monitoring of the reaction at 260 nm. The isotope distribution of the three oxidation products **1**-**3** detected by LC-MS, is consistent with the presence of two chlorine atoms in these products, like in TDMQ20 [intensity ratio of (*m/z* + 2)/(*m/z*) = 66/100, see Figure S1].

Oxidation of TDMQ20 (hydrochloride form, 1 mM) by $KHSO_5$ (4 mol equiv) in aqueous acetonitrile (1/1, v/v) in the absence of catalyst, also produced the expected terminal *N*-oxide **1** as major product (conversion of TDMQ20 = 77%, and yield of **1** = 46% after 1 h). No significant amount of other products was detected.

Catalytic oxidation of TDMQ20 by $KHSO_5$ in the presence of MnTMPyP

In a preliminary experiment, the oxidation of TDMQ20•3HCl (50 μM) in the presence of a catalytic amount of MnTMPyP (1 mol% with respect to TDMQ20) associated to $KHSO_5$ (2 mol equiv added at 5 min) was monitored by kinetic UV-visible analysis. In these conditions, TDMQ20 (λ_{max} = 261 nm) was converted in one or several compounds with absorbance at 251 nm (Figure S2a). This significant hypsochromic shift indicated that oxidation was not restricted to the side chain but also occurred on the quinoline moiety. This reaction has reached a plateau after roughly 15 min in these conditions (20 min after recording start Figure S2b), but started again after addition of 2 additional equiv of $KHSO_5$ (Figure 2a).

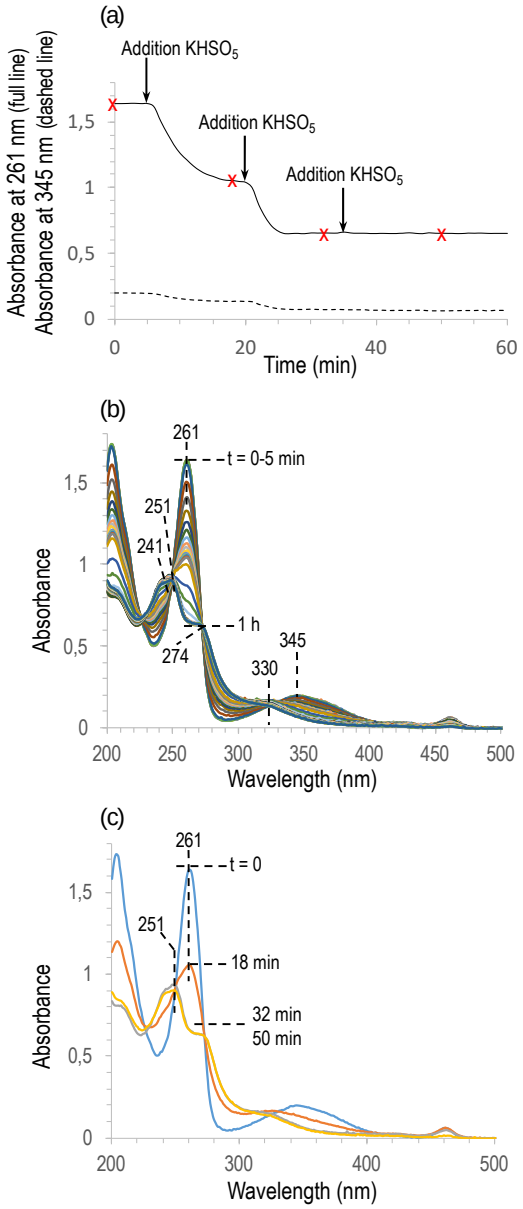

Figure 2. (a) Absorbance at 261 nm and 345 nm according to the reaction time upon three successive additions of $KHSO_5$ (2 mol equiv each) at 5 min, 20 min and 35 min; Spectra at t = 0, 18 min, 32 min and 50 min (red crosses) are depicted in Figure 2c; (b) UV-visible kinetic spectra of the catalytic oxidation of TDMQ20 (50 μM) by three successive additions of $KHSO_5$ 2 mol equiv in the presence of MnTMPyP 1 mol% in H_2O/CH_3CN, 1/1, v/v; time interval between two successive spectra was 1 min; (c) Spectra at t = 0 (blue), 18 min (orange), 32 min (grey) and 50 min (yellow). Absorbance at 462 nm is due to MnTMPyP catalyst.

The maximum wavelength was then shifted at 251 nm with a shoulder at 240-242 nm, indicating that the amount of $KHSO_5$ was the limiting factor of the reaction (Figure 2b and 2c). The oxidation of TDMQ20 was complete after addition of 2 x 2 mol equiv of $KHSO_5$, and no further change was observed after the addition of a third aliquot of oxidant (Figure 2a).

In attempts to isolate the oxidation products of TDMQ20•3HCl by the biomimetic system MnTMPyP/$KHSO_5$, the reaction was carried out at higher concentration (1 mM), and monitored by HPLC with detection by UV-visible (Figure S4) or HRMS (Figure S3).

Measured on UV-vis. chromatogram at 260 nm (Figure S4), the conversion of the substrate was very fast, with a substrate conversion being 52% or 97% after only 1 min in the presence of 1 or 4 mol equiv of oxidant, respectively. After 10 min in presence of 2 mol equiv of $KHSO_5$, the conversion of TDMQ20 was nearly complete (Table 1). In these conditions, *N*-oxidation of the substrate (compounds **1** and **2**) was not detected upon monitoring of the reaction by LC-MS. In fact, six new peaks of this biomimetic oxidation (**4**-**9**) were detected, with retention times ranging from 7.0 to 21.0 min (Figure S4). Consistently with the detection of well-defined isosbestic points at 251, 274 and 330 nm in Figure 2b, UV-visible spectra of all these products were similar (Figure S4), suggesting the formation of several products having similar aromatic moieties. This allowed to calculate their respective proportions according to the reaction time (1 min, 10 min or 1 h) and the amount of oxidant (1 or 4 mol equiv with respect to TDMQ20). Results are reported in Table 1 (and Figure S5) and suggest that both competitive and consecutive reactions occurred in these biomimetic conditions.

The identification of compounds **4**-**9** responsible for the most part of these HPLC peaks was carried out using ESI^+-HRMS (Figure S3). In fact, consistency of HRMS, associated to the specific isotopic patterns of compounds containing one to 5 chlorine atoms, allowed unambiguous determination of the molecular formulas of compounds **4**-**9**. Then, owing to the already reported oxidative reactivity of metalloporphyrins towards aniline and phenol derivatives, reasonable structures could be assigned to these products. The first series of oxidation products corresponds to monoquinoline derivatives **4a**-**4d**, **5** and **6** (Scheme 5). These compounds result from one-electron oxidation of the 8-aminoquinoline ring by the high-valent metalloporphyrin catalyst, leading to a radical cation species. Then, nucleophilic substitution by HO^- leads to hydroquinone **B**, Scheme 6 (compounds **4b**, **4c**, Scheme 5), through 1,4-chlorophenol derivative **A**, Scheme 6, and followed by oxidation of hydroquinone **B** to 1,4-benzoquinone **C** (**4a**, **4d** and **6**, Scheme 5). Oxidative chlorination (structure **D**, Scheme 6; **4d**, **5** and **6**, Scheme 5) or aromatic hydroxylation (structure **E**, Scheme 6; **4b**, Scheme 5) also occurred, probably at C4 which is expected to be the more electrophilic position of the quinoline ring (however, the formation of several position isomers cannot be unambiguously ruled out). The metal catalyzed oxidation of aniline was previously reported to generate 1,4-aminophenol, hydroquinone and *p*-benzoquinone.[19] The oxidative dechlorination at C5, the para position of NH_2, is reminiscent from the first step of oxidative degradation of 2,4,6-trichlorophenol by similar catalytic systems,[20] while oxidative halogenation by biomimetic catalysts has been already reported.[21] In addition, the 2-vinyl derivative **4d** (Scheme 5) was detected. This compound may result from catalytic hydroxylation of the highly oxidizable benzylic position (Quin-C2–*CH_2*; **F**, Scheme 6), followed by dehydration either in the reaction mixture or under mass spectrometry conditions.

Table 1. Oxidation of TDMQ20 in aqueous acetonitrile, in presence of MnTMPyP associated to $KHSO_5$ according to the reaction time and the number of molar equiv of $KHSO_5$.

	Number of mol equiv. of $KHSO_5$	Conversion of TDMQ20[a]	Proportions[b] of chromatographic peaks at					
		R_t [min] = 16.5	**7.0-7.3**	**12.5**	**14.0**	**15.5**	**17.5-17.7**	**21.0**
Reaction time								
1 min	1	52%	10%	26%	47%	8%	5%	nd[c]
	2	77%	10%	26%	49%	8%	4%	nd[c]
	4	97%	15%	20%	45%	9%	9%	<1%
10 min	2	99%	17%	2%	23%	2%	21%	24%
1 h	1	86%	26%	2%	48%	7%	12%	<1%
	2	100%	21%	1%	27%	2%	21%	22%
	4	100%	nd[c]	nd[c]	37%	nd[c]	nd[c]	50%

[a] Calculated with respect to starting amount of TDMQ20, on the basis of HPLC peaks areas at 260 nm; [b] Calculated as (amount of peak n)/Σ amounts of product peaks x 100, based on areas of HPLC peaks at 260 nm (Figure S4). [c] No significant amount (< 1%).

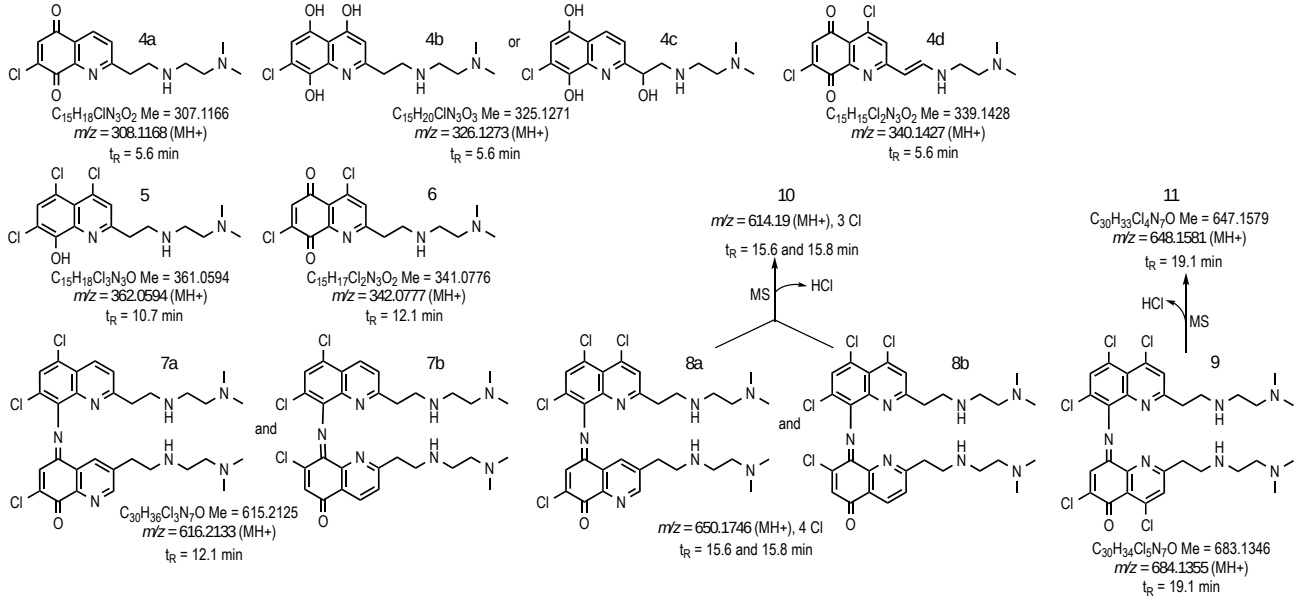

Scheme 5. Proposed structures of the products resulting from oxidation of TDMQ20 in the presence of 1 mol% of MnTMPyP and 1 mol equiv of $KHSO_5$ in H_2O/CH_3CN, 1/1, v/v, 1 h, RT. All compounds were identified by LC-ESI^+-HRMS, except **8a** and **8b** that were identified by ESI^+-low resolution MS. Calculated exact mass values and experimental detected *m/z* values are provided.

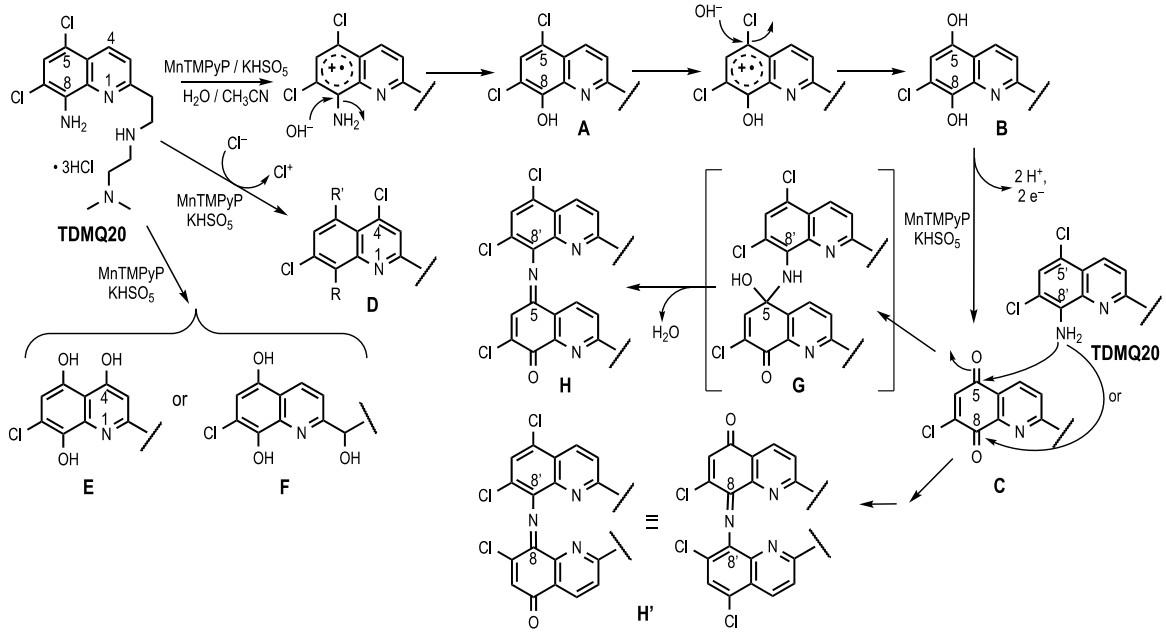

Scheme 6. Proposed mechanisms of oxidation of TDMQ20 by MnTMPyP/$KHSO_5$ in H_2O/CH_3CN. The hydroxylamine intermediate depicted in square brackets was not detected.

A second series of oxidation products **7**-**9** results from the nucleophilic attack of the aniline moiety of TDMQ20 on one of the carbonyl functions of the 5,8-benzoquinone ring resulting from the two-electron oxidation of quinoline ring (**C**, Scheme 6). This reaction yields a series of TDMQ20 dimers linked by a 5,8'- or 8,8'-imine function, and bearing three chlorine substituents (**H** and **H'**, respectively, Scheme 6, compound **7**, Scheme 5).

The dimerization/polymerization of *p*-aminophenol derivatives in the presence of manganese porphyrins associated to $KHSO_5$, was previously reported.[22] The concomitant oxidative chlorination of **7** yielded **8** and **9**. Note that the position of the chlorine atom at C4 and/or C4' is a proposal consistent with the expected reactivity of this position *trans* of the pyridine nitrogen. However, other possible regio-isomers cannot be excluded. The loss of HCl from chlorinated aromatics **8** and **9** in electrospray mass spectrometry generated compounds **10** and **11**, respectively.[23]

Noteworthy, all these dimeric quinone-imine derivatives exhibit similar UV-vis spectra with absorbances at 247-250 nm, 280 nm, 316-317 nm, and a broad band at 497-500 nm (Figure S4). This latter one is in the range reported for a quinone-imine structure.[24]

The various involved reactions (aromatic hydroxylation, oxidation of 1,4-diphenol or 1,4-aminophenol to 1,4-quinone or 1,4-quinone-imine, respectively, oxidative chlorination) are usually performed by P450 enzymes and biomimetic catalytic systems.

Faced to complex reaction mixtures, we tried to isolate the two more abundant products obtained in the presence of 4 mol equiv of $KHSO_5$, in order to characterize them by NMR. After 1 h of reaction time and elimination of the excess of $KHSO_5$ by addition of sodium dithionite ($Na_2S_2O_4$, 4 mol equiv with respect to TDMQ20), the reaction mixture was extracted with dichloromethane, and precipitated by addition of hexane. Alternatively, the reaction mixture was submitted to preparative HPLC. However, in both conditions, products were labile upon work-up conditions.

One can notice that the aniline function of TDMQ20 disappeared in all the oxidation products that have been characterized. Since this amine function was essential in the specific chelation of Cu(II) by TDMQ20,[7,10] the affinity of oxidized derivatives **4**-**9** for Cu might be significantly lower than that of TDMQ20 itself. However, pharmacokinetic studies indicated that, after oral administration of TDMQ20 to rat, bioavailability and brain penetration brain were very high.[25]

Conclusion

TDMQ20 hydrochloride is easily oxidized by a catalytic system mimicking cytochrome P450 and the resulting oxidation products **4**-**9** are fully soluble in aqueous experimental conditions. These data suggest that the drug-candidate TDMQ20 will be metabolized *in vivo* avoiding a possible accumulation in tissues. The isolated distal N-oxide derivative 1 was also highly soluble in aqueous medium at physiological pH. All these data collected on the oxidation products of TDMQ20 might be useful for the identification of the drug-candidate metabolites in future *in vivo* studies.

Experimental Section

Materials and methods.

All solvents and commercially available reagents were purchased from Sigma-Aldrich, Fluka, Acros or Carlo Erba, and used without further purification. Reactions were monitored by thin-layer-chromatography (TLC) by using neutral aluminum oxide plates (Merck). Aqueous solutions were obtained using ultrapure milliQ water. Depending on solvent conditions, two sources of oxone (hydrogen persulfate, named also monopersulfate, HSO_5^-) salt were used for oxidation reactions.

Oxone tetrabutylammonium salt [triple salt of $2NBu_4HSO_5•NBu_4HSO_4•(NBu_4)_2SO_4$] for reactions in dichloromethane and oxone potassium salt [triple salt $2KHSO_5•KHSO_4•K_2SO_4$] for reactions in water/acetonitrile. $Mn(TMPyP)Cl_5$ (MnTMPyP for short) was obtained from Enzo. ^1H and ^{13}C NMR spectra were recorded on Bruker Avance 600 and Avance 400 spectrometers using tetramethylsilane (TMS) as the external standard.

UV-visible conditions. UV/Visible spectra were recorded from 200 to 800 nm on an Agilent Cary 3500 spectrophotometer equipped with magnetic stirrer. For kinetic experiments, spectra were acquired per cycle time of 15 sec or 1 min, under reaction time collection of 1 h.

HPLC conditions. HPLC analyses were carried out using an Agilent 1200 system equipped with a diode array detector and a Waters XBridge C18 column (4.6 x 150 mm, 3.5 µm), eluted with a linear gradient methanol/water/formic acid from 5/95/0.1, v/v/v, to 95/5/0.1, v/v/v, in 24 min; flow rate: 0.5 mL/min, UV detection: 260 and 340 nm.

LC-MS conditions. LC-MS analyses were performed on a Thermo Scientific LCQ Fleet or Waters Xevo-G2QTOF mass spectrometer in positive ionization mode (ESI^+) with the same column under the same gradient conditions as applied for HPLC analysis (see above). The spectra were acquired in *m/z* range 200-1200 or 200-2000 amu; flow rate was 0.5 mL/min.

Preparative HPLC conditions. Purifications were carried out using an autopurification Water 2767 semi-preparative HPLC system equipped with a Waters 2998 photodiode array detector and a Waters XBridge C18 column (19 x 150 mm, 5 µm), eluted with a linear gradient methanol/water/formic acid from 5/95/0.1, v/v/v to 100/0/0.1, v/v/v, in 36 min; flow rate: 20 mL/min, UV detection: 260 nm.

Neutralization of TDMQ20

TDMQ20 free base was obtained by dissolving the TDMQ20•3HCl salt (202 mg, 0.45 mmol) in 30 mL of 5% $NaHCO_3$ aqueous solution, followed by extraction with dichloromethane (3 x 30 mL). The organic layer was dried over Na_2SO_4, filtered and concentrated under reduced pressure to afford the free base as yellow oil (146 mg, 99 % yield). ^1H NMR (600 MHz, $CDCl_3$): δ (ppm) 8.36 (d, ^3J = 8.6 Hz, 1H), 7.46 (s, 1H), 7.39 (d, ^3J = 8.6 Hz, 1H), 3.24 (t, ^3J = 6 Hz, 2H), 3.19 (t, ^3J = 6 Hz, 2H), 2.82 (t, ^3J = 6 Hz, 2H), 2.50 (t, ^3J = 6 Hz, 2H), 2.25 (s, 6H). ^{13}C NMR (151 MHz, $CDCl_3$): δ (ppm) 159.44 (Quin-*C*2), 139.65 (Quin-*C*8), 137.88 (Quin-*C*9), 133.45 (Quin-*C*4), 126.73 (Quin-*C*6), 123.74 (Quin-*C*10), 122.69 (Quin-*C*3), 117.64 (Quin-*C*5), 113.64 (Quin-*C*7), 58.68 [CH_2–$N(CH_3)_2$], 48.56 (Quin–CH_2-CH_2-N), 47.05 (NH–CH_2-CH_2-N), 45.63 [$N(CH_3)_2$], 37.84 (Quin–CH_2). HRMS (ESI+) calcd for $C_{15}H_{21}N_4Cl_2$ ($M+H^+$) 327.1143, found: 327.1145.

Oxidation of TDMQ20 by mCPBA or NBu_4HSO_5 in CH_2Cl_2 in the absence of catalyst

Oxidation of TDMQ20 was carried out by reacting TDMQ20 base (2.78 mg, 8.5 µmol) with 1.2 mole equiv of mCPBA (10.2 µmol) in dichloromethane (850 µL, initial [TDMQ20] = 10 mM), at room temperature. Reaction progress was monitored by TLC on aluminum oxide plates eluted with CH_2Cl_2/4M NH_3 in MeOH (9/1). Alternatively, the reaction was performed with oxone tetrabutylammonium in dichloromethane. Two molar equiv of NBu_4HSO_5 (16.2 µmol) were reacted with TDMQ20 base (2.65 mg, 8.1 µmol) in dichloromethane (810 µL) at room temperature. After 45 min of stirring, full conversion of the substrate was checked by TLC, and the mixture was analyzed by HPLC and LC-MS. Product yields were determined by comparison with TDMQ20 relative absorbance obtained by HPLC with UV detection at 260 nm.

Preparation of TDMQ20 *N*-oxide derivatives 1 and 2

To a solution of TDMQ20 free base (119 mg, 0.36 mmol) in dichloromethane (7 mL) at 0°C was added 1.3 equiv of mCPBA (0.47 mmol). The mixture was stirred at room temperature for 1 h and, then, evaporated under vacuum. The crude yellow residue obtained was purified by chromatography over a neutral alumina column (dichloromethane/4 M NH_3 in MeOH, from 100/0 to 90/10, v/v) to afford the *N*-oxide derivative **1** as a yellow oil (81 mg, 65% yield). ^1H NMR (600 MHz, $CDCl_3$): δ (ppm) 8.34 (d, ^3J = 8.6 Hz, 1H, H4), 7.44 (s, 1H, H6), 7.37 (d, ^3J = 8.6 Hz, 1H, H3), 3.45 [t, ^3J = 5.4 Hz, 2H, (CH_2–$N(O)(CH_3)_2$)], 3.27-3.22 [m, 8H, N(O)–(CH_3)$_2$) + NH–CH_2], 3.22-3.17 [m, 4H, (Quin–CH_2-CH_2-N)]. ^{13}C NMR (151 MHz, $CDCl_3$): δ (ppm) 159.14 (Quin-*C*2), 139.85 (Quin-*C*8), 138.01 (Quin-*C*9), 133.37 (Quin-*C*4), 126.72 (Quin-*C*6), 123.71 (Quin-*C*10), 122.63 (Quin-*C*3), 117.59 (Quin-*C*5), 113.71 (Quin-*C*7), 69.60 [CH_2–$N(O)(CH_3)_2$], 59.77 [$N(O)(CH_3)_2$], 48.64 (Quin–CH_2-CH_2-N), 44.80 (NH-CH_2), 38.11 (Quin–CH_2). HRMS (ESI^+) calculated for $C_{15}H_{21}N_4OCl_2$ ($M+H^+$) 343.1092, found: 343.1096.

Minor oxidation product **2,** bearing two *N*-oxide functions was also purified as a yellow oil (6 mg, 4.6% yield). ^1H NMR (600 MHz, $CDCl_3$): δ (ppm) 8.32 (d, ^3J = 8.6 Hz, 1H, H4), 7.47 (d, ^3J = 8.6 Hz, 1H, H3), 7.43 (s, 1H, H6), 3.63 [m, 2H, (CH_2–$N(O)(CH_3)_2$)], 3.35-3.20 (m, 12H). ^{13}C NMR (151 MHz, $CDCl_3$): δ (ppm) 159.79 (Quin-*C*2), 139.48 (Quin-*C*8), 137.86 (Quin-*C*9), 133.16 (Quin-*C*4), 126.54 (Quin-*C*6), 123.63 (Quin-*C*10), 123.16 (Quin-*C*3), 117.83 (Quin-*C*5), 113.50 (Quin-*C*7), 69.00 [CH_2–$N(O)(CH_3)_2$], 59.39 (Quin–CH_2-CH_2-N), 58.78 [$N(CH_3)_2$], 55.57 [CH_2-CH_2-$N(O)(CH_3)_2$], 36.42 (Quin–CH_2). HRMS (ESI^+) calculated for $C_{15}H_{21}N_4O_2Cl_2$ ($M+H^+$) 359.1042, found: 359.1041.

Kinetic monitoring of TDMQ20 oxidation by $MnTMPyP/KHSO_5$ or by $KHSO_5$ alone in H_2O/CH_3CN, 1/1, v/v

To a cuvette containing TDMQ20•3HCl (15 µL of a 5 mM stock solution, 50 µM in the cuvette, 1 equiv) in presence of MnTMPyP (0.8 µL of a 1 mM stock solution, 0.5 µM in the cuvette, 1 mol% with respect to TDMQ20) in water/acetonitrile, 1/1, v/v, under stirring at room temperature, was added 2 mol equiv or 4 mole equiv of $KHSO_5$ (10 µL of 0.015 M or 0.03 M stock solutions, 100 µM or 200 µM in the cuvette, corresponding to 2 mol equiv or 4 mol equiv, respectively), 5 min after the start of the run. Final volume in the cuvette was 1.5 mL. All stock solutions were prepared in water. UV-visible spectra were recorded as a function of time (cycle time 15 sec, time collection 1 h) from 200 to 800 nm. Similar experiments were also performed with all components except MnTMPyP.

Kinetic oxidation of TDMQ20 by $MnTMPyP/KHSO_5$ with sequential addition of $KHSO_5$

To a cuvette containing TDMQ20•3HCl (15 µL of a 5 mM stock solution, 50 µM in the cuvette, 1 equiv) and MnTMPyP (0.8 µL of a 1 mM stock solution, 0.5 µM in the cuvette, 1 mol% with respect to TDMQ20) in H_2O/CH_3CN, 1/1, v/v, under stirring at room temperature, was added $KHSO_5$ in three portions (3 x 5 µL of a 0.03 M stock solution, 3 x 100 µM in the cuvette, 3 x 2 equiv), at 5 min, 20 min and 35 min after the start of the run (15 min between each addition). Final volume in the cuvette was 1.5 mL. All stock solutions were prepared in water. UV-visible spectra were recorded as a function of time (cycle time 1 min, time collection 1 h) from 200 to 800 nm.

Oxidation of TDMQ20 by $MnTMPyP/KHSO_5$ or by $KHSO_5$ alone in H_2O/CH_3CN, 1/1, v/v

To a solution TDMQ20•3HCl (0.25 µmol, 1 mM, 1 equiv) in presence of MnTMPyP (2.5 nmol, 10 µM, 1 mol % with respect to TDMQ20) in H_2O/CH_3CN, 1/1, v/v, was added 1 equiv, 2 equiv or 4 equiv of $KHSO_5$ (0.25 µmol = 1 mM, 0.50 µmol = 2 mM or 1 µmol = 4 mM). Final volume was 250 µL. Reaction mixture was stirred at room temperature. Stock solutions were prepared in water. After 1 min, 10 min or 1 hour, the mixture was analyzed by HPLC and LC-MS. Experiments without catalyst were also performed in the same conditions.

Table 2. Matching of retention times of the oxidation products of TDMQ20 upon detection in an Agilent 1200 system (detection UV-vis.), and in a Waters Xevo-G2QTOF (detection HRMS).

Upon detection by	Matching of R_t [min]						Depicted in
LC-UV	7.0-7.3	12.5	14.0	15.4	17.5-17.7	21.0	Table 1 Figure S4
LC-HRMS	5.4-5.6	10.7-11.0	12.1	13.5	15.6-15.8	19.1	Scheme S5 Figure S3

Matching of retention times of the oxidation products of TDMQ20 upon detection in an Agilent 1200 system (detection UV-vis.), and in a Waters Xevo-G2QTOF (detection HRMS) is summarized in Table 2.

Supporting Information Summary

Supporting Information contains Figure S1: Oxidation of TDMQ20 by mCPBA 1.2 mol equiv, 15 min. LC-MS monitoring with UV-vis detection at 260 nm. Figure S2: UV-visible kinetic spectra of the catalytic oxidation of TDMQ20 (50 µM) by $KHSO_5$ 2 mol equiv in the presence of MnTMPyP 1 mol% in H_2O/CH_3CN, 1/1, v/v. Figure S3: Catalytic Oxidation of TDMQ20 by Mn(TMPyP)Cl_5 (1 mol%) associated to $KHSO_5$ (2 mol equiv). LC-ESI$^+$-HRMS for compounds **4**-**9** after 1 h of reaction. Figure S4: Catalytic Oxidation of TDMQ20 by Mn(TMPyP)Cl_5 (1 mol%) associated to $KHSO_5$ (2 mol equiv). LC-UV-vis. for compounds **4**-**9** after 1 h of reaction. Figure S5: Catalytic Oxidation of TDMQ20 by Mn(TMPyP)Cl_5 (1 mol%) associated to $KHSO_5$. Quantification of reaction products on the basis of HPLC chromatograms with detection at 260 nm.

Acknowledgements and funding sources

This work has been supported by the CNRS, France, and by the University of Technology of Guangdong, China.
Nathalie Martins (Mass spectrometry facilities of the Institute of chemistry of Toulouse, ICT, UAR 2599), and Isabelle Fabing (UMR 5068 CNRS-University of Toulouse) are acknowledged for help with LC-MS analyses and preparative HPLC, respectively.

Keywords: Alzheimer's disease • catalytic oxidation • copper chelator • metabolism

[1] J. L. Cummings, T. Morstorf, K. Zhong, *Alzheimer's Res. Ther*. **2014**, *6*, 37−43.
[2] Editorial, *Lancet* **2010**, *376*, 658.
[3] R. J. Castellani, G. Perry, *Arch. Med. Res*. **2012**, *43*, 694–698.
[4] Y. Liu, M. Nguyen, A. Robert, B. Meunier, *Acc. Chem. Res.* **2019**, *52*, 2026-2035, and references therein.
[5] M. Jakaria, A. A. Belaidi, A. Bush, S. Ayton, *J. Neurochem*. **2021**, *159*, 804–825.
[6] S. J. C. Lee, E. Nam, H. J. Lee, M. G. Savelieff, M. H. Lim, *Chem. Soc. Rev*. **2017**, *46*, 310–323.
[7] W. Zhang, D. Huang, M. Huang, J. Huang, D. Wang, X. Liu, M. Nguyen, L. Vendier, S. Mazères, A. Robert, Y. Liu, B. Meunier, *ChemMedChem* **2018**, *13*, 684-704.
[8] Y. Liu, X. Liu, D. Huang, M. Huang, D. Wang, M. Nguyen, A. Robert, B. Meunier, Chinese Patent 201610369550.X, 27 May 2016. WO 2017/202360 A1.
[9] J. Huang, M. Nguyen, Y. Liu, A. Robert, B. Meunier, *Eur. J. Inorg. Chem.* **2019**, 1384-1388.
[10] Y. Li, M. Nguyen, M. Baudoin, L. Vendier, Y. Liu, A. Robert, B. Meunier, *Eur. J. Inorg. Chem.* **2019**, 4712–4718.
[11] M. Nguyen, L. Rechignat, A. Robert, B. Meunier, *ChemistryOpen* **2015**, *4*, 27-31.
[12] M. Nguyen, L. Vendier, J.-L. Stigliani, B. Meunier, A. Robert, *Eur. J. Inorg. Chem.* **2017**, 600-608.
[13] J. Huang, M. Nguyen, Y. Liu, A. Robert, B. Meunier, *Eur. J. Inorg. Chem.* **2019**, 1384-1388.
[14] J. Zhao, Q. Shi, H. Tian, Y. Li, Y. Liu, Z. Xu, A. Robert, Q. Liu, B. Meunier, *ACS Chem. Neurosci.* **2021**, *12*, 140-149.
[15] F. Sun, J. Zhao, H. Zhang, Q. Shi, Y. Liu, A. Robert, Q. Liu, B. Meunier, *ACS Chem. Neurosci*. **2022**, *13*, 3093–3107.
[16] a) B. Meunier, A. Robert, G. Pratviel, J. Bernadou, *Metalloporphyrins in catalytic oxidations and oxidative DNA cleavage*, in *The Porphyrin Handbook*, Eds.: K. M. Kadish, K. M., Smith, R. Guilard, Academic Press, **2000**, vol. 4, pp 119-187; b) B. Meunier, S. P. de Visser, S. Shaik, *Chem. Rev.* **2004**, *104*, 3947-3980; c) X. Huang, J. T. Groves, *Chem. Rev.* **2018**, *118*, 2491-2553.
[17] a) J. Bernadou, B. Meunier, *Adv. Synth. Catal.* **2004**, *346*, 171-184; b) M. Vidal, M. Bonnafous, S. Defrance, P. Loiseau, J. Bernadou, B. Meunier, *Drug Metab. Dispos.* **1993**, *21*, 811-817; c) N. Gaggero, A. Robert, J. Bernadou, B. Meunier, *Bull. Soc. Chim. Fr.* **1994**, *131*, 706-712; d) I. Nicolas, C. Bijani, D. Brasseur, G. Pratviel, J. Bernadou, A. Robert, *C. R. Chimie* **2013**, *16*, 1002-1007.
[18] M.-N. Paludetto, C. Arellano, F. Puisset, V. Bernardes-Génisson, A. Robert, *J. Med. Chem.* **2018**, *61*, 7849-7860.
[19] a) C. Ferreiro, N. Villota, J. I. Lombraña, M. J. Rivero, *Water* **2020**, *12*, 3448; b) J. Barbier Jr., L. Oliviero, B. Renard, D. Duprez, *Top. Catal.* **2005**, *33*, 77-86.
[20] a) A. Sorokin, B. Meunier, *Chem. Eur. J.* **1996**, *2*, 1308-1317; b) B. Meunier, A. Sorokin, *Acc. Chem. Res.* **1997**, *30*, 470-476.
[21] a) B. De Poorter, M. Ricci, O. Bortolini, B. Meunier, *Tet. Lett.* **1985**, *3*1, 221-224; b) W. Liu, J. T. Groves, *J. Am. Chem. Soc.* **2010**, *132*, 12847-12849.
[22] J. Bernadou, M. Bonnafous, G. Labat, P. Loiseau, B. Meunier, *Drug Metab. Dispos.* **1991**, *19*, 360-365.
[23] J. K. Prasain, R. Patel, M. Kirk, L. Wilson, N. Botting, V. M. Darley-Usmar, S. Barnes, *J. Mass Spectrom.* **2003**, *38*, 764-771.
[24] G. Meunier, B. Meunier, *J. Biol. Chem.* **1985**, *260*, 10576-10582.
[25] L. Huang, Y. Zeng, Y. Li, Y. Zhu, Y. He, Y. Liu, A. Robert, B. Meunier, *Pharmaceutics* **2022**, *14*, 2691.

Entry for the Table of Contents

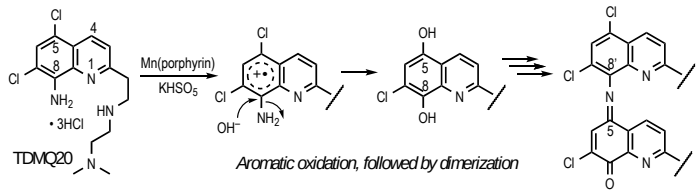

TDMQ20, a drug-candidate against Alzheimer's disease, is easily oxidized in biomimetic conditions, suggesting that it should be readily metabolized *in vivo*, and that potentially deleterious accumulation in tissues should be avoided.